Study of Morphology Influence on Rheological Properties of Compatibilized TPU/SAN Blends

M. Ulcnik-Krump

Center for Experimental Mechanics, University of Ljubljana, Ljubljana, Slovenia

Received 11 March 2005; accepted 13 August 2005
DOI 10.1002/app.22920
Published online in Wiley InterScience (www.interscience.wiley.com).

ABSTRACT: The compatibilizing efficiency of three different compatibilizers on the thermoplastic polyurethane/styrene-*co*-acrylonitrile (TPU/SAN) blends properties was investigated after compatibilizer's incorporation via melt-mixing. The compatibilizers studied were as follows: poly-ε-caprolactone (PCL) of different molecular weight (M_w), a mixture of polystyrene-*block*-polycaprolactone (PS-*b*-PCL) and polystyrene-*block*-poly (methyl methacrylate) (PS-*b*-PMMA), and a mixture of polyisoprene-*block*-polycaprolactone (PI-*b*-PCL) and polybutadiene-*block*-poly (methyl methacrylate) (PB-*b*-PMMA). In our study, the effect of 5 wt % added compatibilizers on TPU/SAN blends morphology was examined. The transmission electron microscopy (TEM) was used to study the morphology at different length scales and to determine the compatibilizer's location. Investigations showed the different improvement of properties, because of the different incorporation of compatibilizers in the polymer blend. The morphology influence on the rheological behavior of compatibilized blends was investigated with a stress-controlled rheometer (Rheometric Dynamic Stress Rheometer, SR-500). Different compatibilization activity was found for different system. It was also found that compatibilization activity of added compatibilizer strongly depends on the comaptibilizer's M_w. Blends compatibilized with PCL showed superior properties as compared with the other examined blends. J Appl Polym Sci 100: 2303–2316, 2006

Key words: compatibilization; blends; morphology; rheology

INTRODUCTION

The design and synthesis of new polymers for specific applications is a time consuming and an expensive process. A successful alternative for the development of new polymeric materials is blending of already existing polymers to obtain a balance (or even synergism) of the desired properties exhibited by the individual components. To improve the performance of immiscible blends, usually polymer additives, so-called "compatibilizers" are added. While miscibility has a strict thermodynamic meaning, compatibility is defined in operational terms. A blend may be more or less compatible, if it is closer or further away from miscibility. The highest degree of compatibility i.e., miscibility, does not always mean the best engineering properties.[1] Good properties are usually achieved with controlled level of phase separation and a stable morphology.[2] Block copolymers, graft copolymers, or functional polymers can be used as compatibilizers.[3] When block or graft copolymers are used as compatibilizers, an efficient mechanical coupling, "wet brush," can only be achieved when each block of the block copolymer intimately mixes with one of the blend components. Our hypothesis was that a homopolymer can also be used as compatibilizer, if it has a sufficient level of compatibility towards both polymer A as well as polymer B blend components.[4] The theoretical background is explained in detail somewhere else.[5] However, homopolymer C can be localized at the interface between polymer A and polymer B, only if the level of compatibility between homopolymer C and polymer A as well as homopolymer C and polymer B is higher than compatibility between polymer A and polymer B. Homopolymer C miscible with each component of the blend might be partitioned between the components, according to some partition coefficient regulated by its relative miscibility with the polymers of the blend. The addition of homopolymers with too large molecular weights can lead to the formation of independent homopolymer phases embedded in the phases of polymer A or polymer B. Less problems with insufficient mechanical coupling are expected if a homopolymer used as a possible compatibilizer for a polymer A/polymer B blend is chemically different but thermodynamically miscible with both of the blend components. But if a block copolymer is used as compatibilizer, then each block of the block copolymer (C-*b*-D) should be chem-

Correspondence to: M. Ulcnik-Krump (manica.ulcnik-krump@guest.arnes.si, cem@fs.uni-lj.si).

Contract grant sponsors: Ministry of Education, Science and Sport, Republic of Slovenia, BMBF/BASF, ESPE, and DFG.

ically different but selectively thermodynamically miscible with one of the blend components. The negative enthalpic interactions between A/C and B/D or A/C and B/C enforce interpenetration at the respective phase boundaries resulting in a "wet brush" situation. In addition, the location of the homopolymer (C) or block copolymer (C-*b*-D) at the A/B interface is thermodynamically favored in comparison to the formation of independent phases of homopolymer (C) or block copolymer micelles. In general, the efficiency of compatibilizers is determined by their preferential location at the interface.[1] However, the use of compatibilizers for a polymer A/polymer B blend does not always result in an improvement of the mechanical phase adhesion. The influence of compatibilizer concentration on the compatibilizing effect should be also taken into account.[6]

The morphological investigation is a key component in the development of any compatibilizer.[1] Both the experimental observations[7–9] and theoretical predictions[10] indicate a reduction in the interfacial tension between immiscible phases in compatibilized polymer blends and a consequent reduction in the dispersed phase domain size. In addition, the presence of a compatibilizer at the interface broadens the interfacial region through penetration of the compatibilizers into adjacent phases. Perhaps more important than reduction in the interfacial tension is the stabilization against coalescence during blending also caused by the location of the compatibilizers at the interface.[11,12]

Rheological properties of compatibilized polymer blends are strongly influenced by the morphology of these materials, which depends on the compatibilizer location in the polymer matrix. The formation of polymer blend morphology[13] and its response to applied shear are scientifically challenging and important to industry processing. To obtain a satisfactory understanding of rheological behavior of polymers, generally data over a wide range of frequencies are required. These frequencies are often outside the experimental window and both frequency and temperature are normally varied. Applying the time–temperature superposition (TTS) principle,[14] master curves that cover a much broader frequency window can be obtained. They are important in predicting the viscoelsatic behavior of a polymer outside the frequencies range (or time) for which experimental data are available and they give a direct indication of what might be expected at other times at that temperature. There are many contradictory discussions about the possibility of using the TTS principle and about the Williams, Landel, Ferry (WLF) equation to generate master curves for thermorheologicaly complex materials. Tschogel and coworkers[15,16] developed a method for constructing a master curve for any two-phase system, where empirical shifting can only yield one shift factor curve and one master curve for a particular reference temperature. In spite of the fact that immiscible polymer blends are not, strictly speaking, thermorheologicaly simple materials, Monge and coworkers[17,18] used the WLF equation to generate master curves of commercial polymer blends.

By blending thermoplastic polyurethane (TPU) with styrene-*co*-acrylonitrile (SAN) many different properties can be achieved because of the numerous commercially available polyurethanes (different raw materials, hard and soft segment composition and ratio, domain separation, etc.) and different SAN copolymers (weight % of acrylonitrile (AN) and different distributions of styrene and AN). Mixing of TPU and SAN can be a successful way to obtain new materials with good properties. The expected synergistic effects of TPU/SAN blending are mainly increasing of SAN toughness and improving thermal stability of TPU. However, TPU/SAN blends are known to be immiscible in the whole composition range,[19–21] but some studies showed a weak interaction between TPU hard segment and SAN.[22] Properties of TPU/SAN blends prepared from solutions were investigated previously.[23] It was established that TPU/SAN blends are immiscible within the entire composition range and the studies of dielectric properties proved phase separation in TPU.[24]

However, in spite of numerous publications in the field of compatibilization of different polymer pairs and many research activities of different research groups headed by Mac Knight, Mewis, Macosko, Friederich, and others, the compatibilized mixtures of TPU and SAN were insufficiently investigated. As described in the patent,[25] Van Cleve, Armstrong, and Simroth prepared a stable dispersion of SAN in TPU by copolymerizing a telechelic poly(propylene oxide) carrying acrylic or methacrylic ester-end groups into the SAN latex. The poly(propylene oxide) chains connected to SAN chains formed the compatibilizer. As potential compatibilizers we used:

- Homopolymer that was known to be compatible with SAN as well as TPU;
- The mixture of compatible block copolymers where one block of mixture was expected to be compatible with SAN and other block of mixture was expected to be compatible with TPU.

According to many published results,[1,26–31] the following polymer additives may also be expected to act as compatibilizers for immiscible SAN and TPU with polyester soft segment:

- Poly-ε-caprolactone (PCL) of different M_w further marked as *C1a*, *C1b*, or *C1c*, where the compatibility between PCL and TPU soft segments as well as between PCL and SAN was expected.[1,26–29] While C1 is expected to be compatible with both

TPU as well as SAN, we suppose that C1 may be located at the TPU/SAN interface to tower interfacial tension. But it is also possible that, depending on PCL molecular weight (M_w), undesirable independent phases of PCL are formed in the SAN phases and in TPU soft segment domains.[4,5]

- Mixture of block copolymers polystyrene-*block*-poly(ε-caprolactone) (PS-*b*-PCL) and polystyrene-*block*-poly(methyl methacrylate) (PS-*b*-PMMA) (PS-bPCL:PS-*b*-PMMA = 50:50) further marked as *C2*, where the compatibility of the polystyrene blocks, the TPU soft segments with the PCL block of PS-*b*-PCL, and the SAN with the PMMA block of PS-*b*-PMMA was expected.[30,31] We presumed that C2 would be located at the TPU/SAN interface. No published results about miscibility between PMMA and TPU were found. Therefore, independent phases of block copolymers mixtures or micelles formed at concentrations larger than the corresponding CMC are expected to be localized in the SAN phase only.
- Mixture of block copolymers polyisoprene-*block*-poly(ε-caprolactone) (PI-*b*-PCL) and polybutadiene-*block*-poly(methyl metacrylate) (PBD-*b*-PMMA) (PI-*b*-PCL: PBD-*b*-PMMA = 50:50) further marked as *C3*, where the compatibility between polyisoprene and polybutadiene blocks of the copolymers, between TPU soft segments and the PCL block of PI-*b*-PCL, and between SAN and the PMMA block of PB-*b*-PMMA was presumed.[30,31] C3 is expected to be located at the TPU/SAN interface.

While changes in thermal and thermomechanical properties are often used as basic information and as an evidence of compatibilizer efficiency in compatibilized polymer blends, the differential scanning calorimetry (DSC) and dynamic mechanical thermal analysis (DMTA IV) were used for preliminary investigation of compatibilization efficiency of proposed compatibilizers.[5]

EXPERIMENTAL

Materials

Commercial thermoplastic polyurethane (TPU) and styrene-*co*-acrylonitrile (SAN) supplied BASF (Ludwigshafen, Germany) were selected as the basic components for the polymer blends. The AN content in SAN was 20 wt %, as determined by elemental analysis. The analysis of the ^{1}H NMR spectrum of the TPU showed that the hard segment phases were built from 4,4-diphenylmethane diisocyanate (MDI) and 1,4-butanediol (BD) and the soft segment phases were synthesized from adipic acid and hexamethylene glycol. All polymers used as compatibilizers were synthesized by living anionic polymerization. The details are explained somewhere else.[4,5]

The relative molecular weights (M_w and M_n) and the polydispersity (PI) of compatibilizers as well as polymers used as matrix were determined by SEC in THF at 40°C, using PS standards for calibration. The measurements were performed in an instrument equipped with PL-gel columns (Bischoff). The refractive index and the UV absorption (254 nm) were monitored by a differential refractometer and a UV-detector (Waters), respectively. ^{1}H NMR spectra were obtained at room temperature on a Brukner AC-200 spectrometer. $CDCI_3$ was used as solvent for all the polymers. Materials descriptions including basic molecular characteristics and thermal properties as obtained by DSC are summarized in Table I.

Sample preparation

Before blending, TPU and SAN were dried for at least 48 h under vacuum at 100°C to minimize hydrolysis during processing. Blending was performed using a corotating twin-screw mixer with conical screws, developed in the TU Eindhoven, Netherlands. After complete feeding, the material was kept in the mixer for ~2 min. The screw speed was 30 rpm. Mixing was performed under dry nitrogen. Approximately 3 g of materials was used to obtain optimal mixing conditions. TPU/SAN 25/75 blends with 5 wt % of compatibilizer were prepared. The samples were, after blending in the twin-screw mixer, placed in a hydraulic press and molded into a metal-steel disk with a diameter of 25 mm and 1 mm thick at 180°C, under pressure of 10 kPa for 5 min.

Microscopy

Micrographs were taken with a CEM 902 Zeiss transmission electron microscope (TEM), with an accelerating voltage of 80 kV. The microscope is equipped with an energy filter system based on casting filter.

Compatibilized and noncompatibilized TPU/SAN 25/75 blends were annealed for 10 days at 100°C before the samples were prepared for TEM. For the similar system, Groeninckx and coworkers[32] observed that parallel and perpendicular surfaces of annealed samples exhibit the same morphology. Therefore, the phase morphology was monitored only on sheets cut perpendicular to the extrusion flow direction. The sections were cut with a cryoultrarmicrotom Ulratacut E Reichert-Jung at −60°C, using a diamond knife and were mounted on copper greed.

According to Eckert-Rectanus,[33] an anionic phosphotungistic acid (PTA) with M_w = 3313.5 g mol^{-1} can be used for staining SAN. Hayat[34] described a possible mechanism of staining with PTA. Therefore, noncompatibilized and compatibilized TPU/SAN 25/75

TABLE I
Descriptions of Materials Used Including Basic Molecular Characteristics and Thermal Properties Obtained by DSC

Material denotation	Acronym[a]	$M_w \times 10^{3b}$ (g/mol)	PI = $\frac{M_w}{M_n}$[c]	Thermal analysis[d] (°C)
	TPU	160	2.3	T_g (TPU) = −46.0
	SAN	170	2.4	T_g (SAN) = 109.0
C1a	PCLa	104	1.3	T_g (PCLa) = −61.3
C1b	PCLb	87	1.2	T_g (PCLb) = −61.5
C1c	PCLc	49	1.4	T_g (PCLc) = −57.2
	$PS_{30}PCL_{70}^{65}$	65	1.3	T_g (PCL) = −56.4
C2				T_g (PS) = 85.0
	$PS_{24}PMMA_{76}^{78}$	78	1.2	T_g (PS) = 89.4
				T_g (PMMA) = 117.3
	$PB_{29}PMMA_{71}^{105}$	105	1.1	T_g (PB) = −61.7
C3				T_g (PMMA) = 115.3
	$PI_{65}\ PCL_{35}^{137}$	137	1.2	T_g (PI or PCL) = −58.3

[a] Acronym of synthesized polymers.

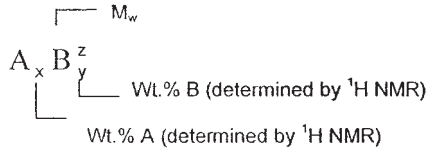

M_w, obtained by SEC relative to PS standard; x, wt % of block A determined by ^{1}H NMR; and y, wt % of block B determined by ^{1}H NMR.
[b] Obtained by SEC relative to PS standard.
[c] Obtained by SEC relative to PS standard.
[d] Obtained by DSC and calculated as an average value of at least three measurements.

blends were stained with a 4 wt % aqueous solution of PTA (Aldrich) for 5–7 min at 60°C and then washed at least three times with distilled water.

Rheology investigations

Rheology investigations were performed using the Rheometric Dynamic Stress Rheometer (SR-500). Either sinusoidal (dynamic) or linear (steady and transient) stresses can be applied to the sample. Equipment control, data acquisition, and treatment are made by RSI Orchestrator software.[35] Stress was applied by the stress head, a rotatory actuator attached to a precision air bearing. A position sensor mounted on the stress head outputs the strain, the angular deflection of the stress head. Calculation of the polymer properties was performed by analysis of the applied stress and the resulting strain. The gap used in the experiments was always between 0.7 and 0.8 mm.

Isothermal frequency sweeps were recorded between 130 and 220°C in steps of 10°C to obtain master curves. Further increase in the temperature was impossible because of the thermal instability of the samples. The frequency was varied between 100 and 10^{-2} rad s^{-1}. The region of linear viscoelastic behavior was determined performing stress sweeps.

All creep experiments were performed in parallel plate geometry with diameter 25 mm at 140°C. To prevent chemical reactions at this temperature, all tests were performed under dry nitrogen. The region of linear viscoelastic behavior of the materials was determined by a standard test in the Orchestrator software. The stress used in all experiments was 10 kPa and was within the region of linear viscoelastic behavior of all materials. Before performing the measurements, samples were annealed for 12 h at 140°C placed into Stress Rheometer under dry nitrogen. The creep experiments were performed for a period of 600 min.

The viscosity and compliance values were calculated using the Rhios software functions in *creep analysis*, which provides tools to examine data in the steady state regions of both creep and recovery zones.[35] The *flow term* function calculates the steady state viscosity of the creep experiment. The software searches for the variables of creep compliance ($J(t)$), stress (σ), and time (t) automatically and divides the curve into windows as shown in Figure 1. Starting from the end of the curve and working toward time zero, a least square fit is performed in each window and the slope of the curve is calculated. The program considers that the steady state has been reached when the difference between the slopes calculated for two adjacent windows is less than the slope tolerance (the default value for slope tolerance is 10%). The straight line resulting from the least square fit in the steady state region is extrapolated to time zero. The interception with the y-axis is the steady-state compliance (J_0).

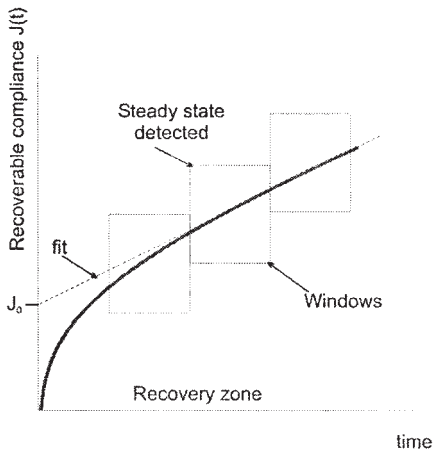

Figure 1 Schematically shown determination of J_0.

RESULTS AND DISCUSSION

Morphology

The phase morphology of typical noncompatibilized and compatibilized TPU/SAN 25/75 blends is presented in Figure 2(a–f). The dispersion of phases is dependent on a number of different parameters. Some irregularities and defects in micrographs are a consequence of the difficulties that occurred during sample preparation. Even small differences in thickness, which can result from small variations in the cutting temperature, create contrast differences and might hide the real structure. The matrix (continuous dark phase) formed by the major component SAN (75 wt %) and disperse (discontinuous light phase) TPU phase are present in all micrographs. It is seen that the size and shape of the TPU domains are not uniform. We presume that this also partly reflects the blending conditions (screw speed, temperature, and blending sequence).

In Figure 2(a), the TEM micrograph of the noncompatibilized TPU/SAN 25/75 blend is shown. Two phases can be seen, demonstrating clearly that TPU and SAN form an incompatible blend. The boundaries between the TPU and the SAN phases are not distinct. Following the theory of Utracki,[36] this interfacial region can be considered as an interphase; a third phase in the immiscible blends with its own characteristic properties. The thickness of the interphase layer depends on thermodynamic interactions, macromolecular segment size, concentration, and phase condition. In general, indistinct boundaries can be described as a fine dispersion, indicating that TPU and SAN can be partly miscible.

Figure 2(b–d) show the micrographs of TPU/SAN 25/75 blends compatibilized with PCL of different M_w [Fig. 2(b)] TPU/SAN 25/75 blend with 5 wt % of PCL with M_w = 104,000 g mol^{-1} (C1a), Figure 2(c) TPU/SAN 25/75 blend with 5 wt % of PCL with M_w = 89,000 g mol^{-1} (C1b), and Figure 2(d) TPU/SAN 25/75 blend with 5 wt % of PCL with M_w = 49,000 g mol^{-1} (C1c)). It can be clearly seen that the size of the TPU domains in blend with added C1a [Fig. 2(b)] are larger than in noncompatibilized blend [Fig. 2(a)]. The boundaries between phases are also more distinct than in noncompatibilized blends. Because of the formation of independent phases of C1a in the SAN matrix as it was determined with DMTA,[5] it is expected that the addition of C1a influences the viscosity of matrix, which consequently increases the size of the dispersed phase.

In Figure 2(c), it can be seen that in the case of C1b, the compatibilizer is located at the interphases between TPU and SAN. Obviously, added C1b does not

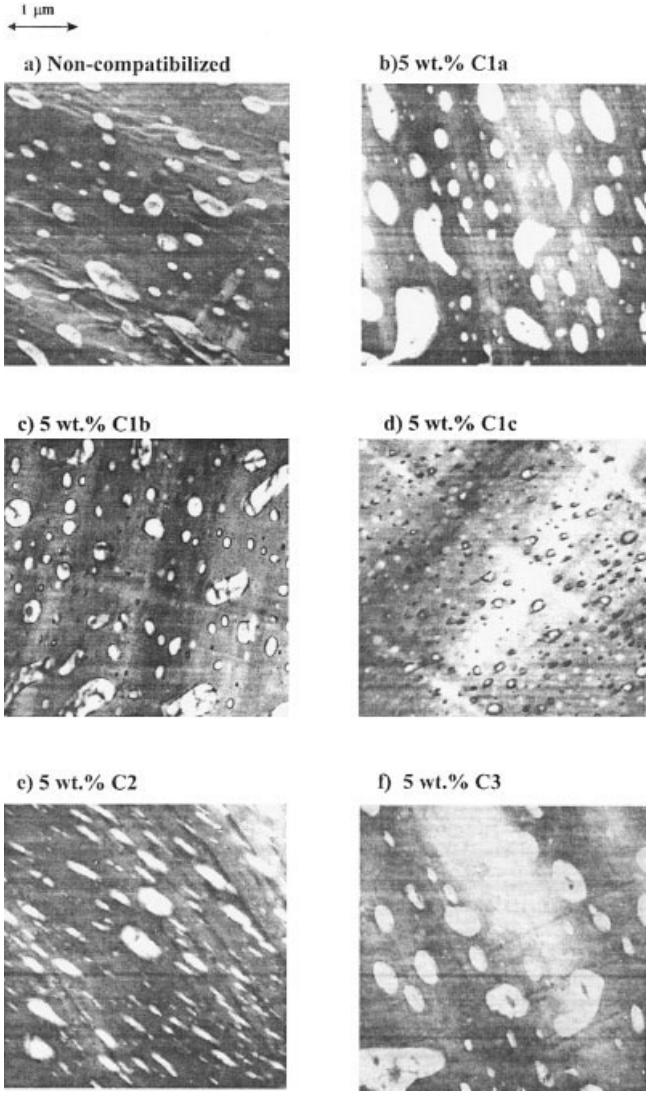

Figure 2 TEM micrographs (a) noncompatibilized TPU/SAN 25/75 blend, (b) TPU/SAN 25/75 blend compatibilized with 5 wt % of C1a, (c) TPU/SAN 25/75 blend compatibilized with 5 wt % of C1b, (d) TPU/SAN 25/75 blend compatibilized with 5 wt % of C1c, (e) TPU/SAN 25/75 blend compatibilized with 5 wt % of C2, and (f) TPU/SAN 25/75 blend compatibilized with 5 wt % of C3.

reduce the size of the dispersed phase, but probably improves the stabilization against coalescence. It is evident in Figure 2(d) that the addition of C1c causes a large decrease in the size of the TPU domains. Additionally, a layer of C1c with indistinct boundaries is clearly seen at the TPU-SAN interphases. The addition of compatibilizer C2 (mixture of PS-*b*-PCL and PS-*b*-PMMA) influences the shapes of the dispersed domains, which are more ellipsoidal [Fig. 2(e)] in contrast to more spherical domains in the noncompatibilized blend [Fig. 2(a)]. The boundaries between phases are not distinct. The morphology of the blend with compatibilizer C3 (mixture of PB-*b*-PMMA and PI-*b*-PCL) as illustrated in Figure 2(f) is quite similar to the one of noncompatibilized blend. In the micrographs of the blends compatibilized with C3, it is not possible to identify separated compatibilizer phase, as it was observed in the DMTA measurements.[5] Our speculation is that C3 is distributed through the sample on the molecular size level and in that case some blocks of C3 (PI and PB) that can also react with PTA remain partly undetected in the SAN matrix.

Determination of domain size

Domain size determination in polymer blends is usually performed using image analysis, where the cross-sectional area of all particles present in the micrograph is measured. Generally, it is assumed that all particles of the dispersed phase are circles and that the error associated with this assumption is negligible. Because of this simplification, the measured particle areas can be converted to particle diameters (d). A size correction can be done using the Cruz-Orive[37] method. Macosko and Sundararaj[38] showed that it is possible to use it for the calculation of domain size in polymer blends. They compared the corrected values with the raw data, and the difference in the average particle size was less than 10%. In the micrographs, the particles are two-dimensional and their areas and diameters are related by the equation. It was assumed that all particles of the dispersed phase are circles and that the error associated with this assumption is negligible. Because of this simplification, the measured particle areas can be converted to particle diameters (d). In the micrograph, the particles are two-dimensional and their areas and diameters are related by the eq. (1).

$$d = \sqrt{\frac{4(\text{arca})}{\pi}} \tag{1}$$

and the apparent radius (r) is given by

$$r = \frac{d}{2} \tag{2}$$

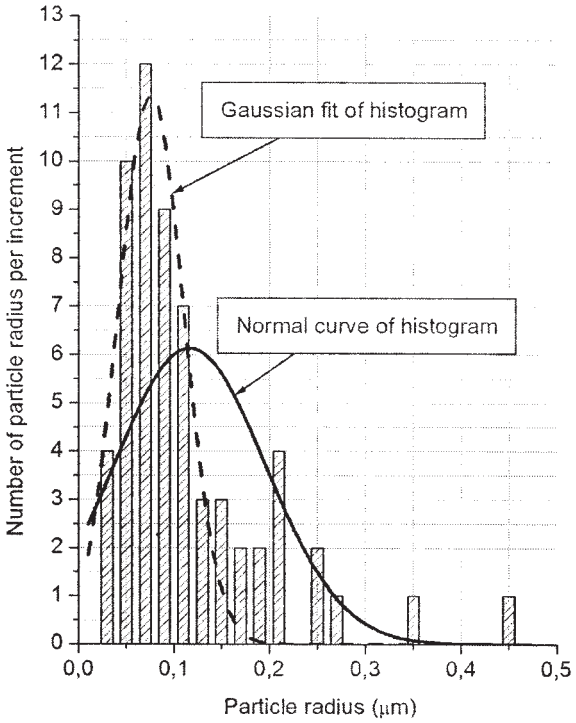

Figure 3 Histogram of TPU size distribution for a typical TPU/SAN 25/75 blend.

But in reality, the domains are three-dimensional and they can be sectioned at any plane,[39] not necessarily always through the center. Wu[40,41] proposed that if the particles are randomly distributed, the true particle size distribution function $f(a)$ is related to the observed apparent particle size distribution function $f(r)$:

$$f(r) = \int_0^\infty f(a)g(r,a)\, da \tag{3}$$

where a is the true radius and

$$g(r,a) = \left(\frac{r}{a}\right)\sqrt{(a^2 - r^2)} \text{ for } r < a \tag{4}$$

$$g(r,a) = 0 \text{ for } r > a \tag{5}$$

Inversion gives $f(a)$ and finally the observed average radius $\bar{r}$ is given by eq. (6):

$$\bar{r} = \left(\frac{\pi}{4}\right)a \tag{6}$$

Based on the finding published by Ghodgaonkar et. al.,[42] it was anticipated that Cruz-Orive size corrections could be neglected. Figure 3 shows the histograms of noncompatibilized compatbilized TPU/SAN 25/75 blends pre-

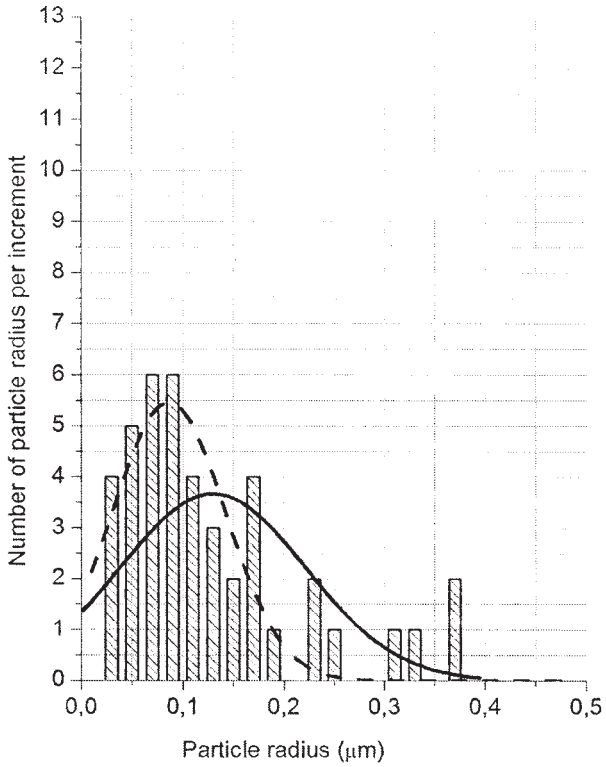

Figure 4 Histogram of TPU size distribution for a typical TPU/SAN 25/75 blend compatibilized with Cla.

sented in Figure 2(a–f). To get the reliable statistics, histograms were obtained from analyzes of at least three micrographs of each sample. The corresponding curves of the normal and Gaussian distributions are also shown. The comparison of Gaussian and normal distribution curves of blends compatibilized with different compatibilizers is shown in Figure 4(a,b). The mean values of the domain radius of blends calculated by the eqs. (1–6) are summarized in Table II.

The influence of the molecular weight of compatibilizers C1a, C1b as well as C1c on the morphology of the blends can be clearly seen in the Figures 5–7. The

TABLE II
The Values of Observed Average Radius of Dispersed TPU Domains for Noncompatibilized and Compatibilized TPU/SAN 25/75 Blends

TPU/SAN 25/75 +5 wt % compatibilizer	$\bar{r}$	
	Obtained as mean point of normal curves (μm)	Obtained as mean point of Gaussian curves (μm)
None	0.13	0.07
C1a	0.16	0.12
C1b	0.12	0.09
C1c	0.07	0.06
C2	0.13	0.11
C3	0.15	0.11

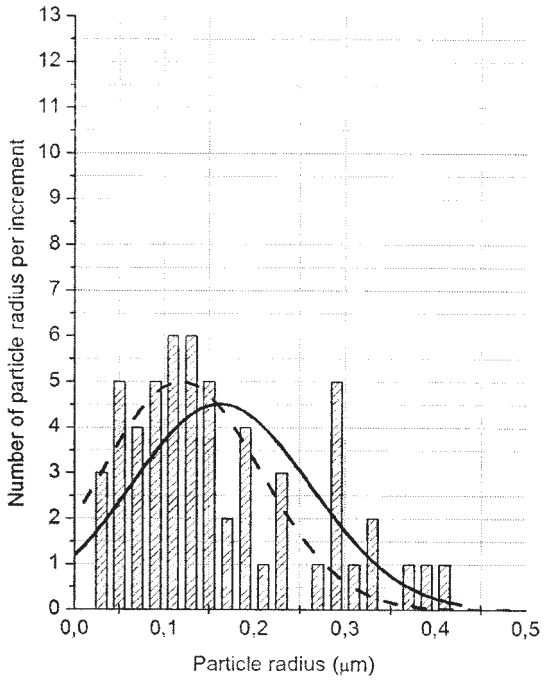

Figure 5 Histogram of a TPU size distribution for a typical TPU/SAN 25/75 blend compatibilized with C1b.

increase in the size of the dispersed TPU domains and the sharper boundaries between phases indicate that C1a (PCL with the highest M_w) presumably causes coalescence, while the addition of C1c (PCL with the lowest M_w) reduces the size of the dispersed TPU domains.

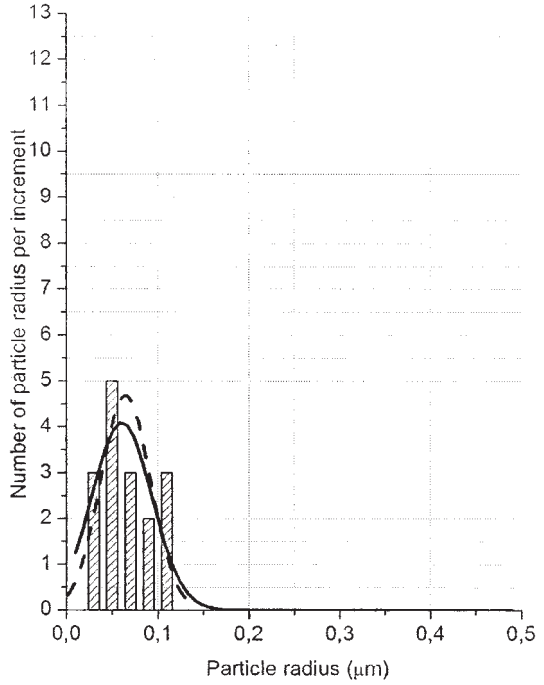

Figure 6 Histogram of a TPU size distribution for a typical TPU/SAN 25/75 blend compatibilized with C1c.

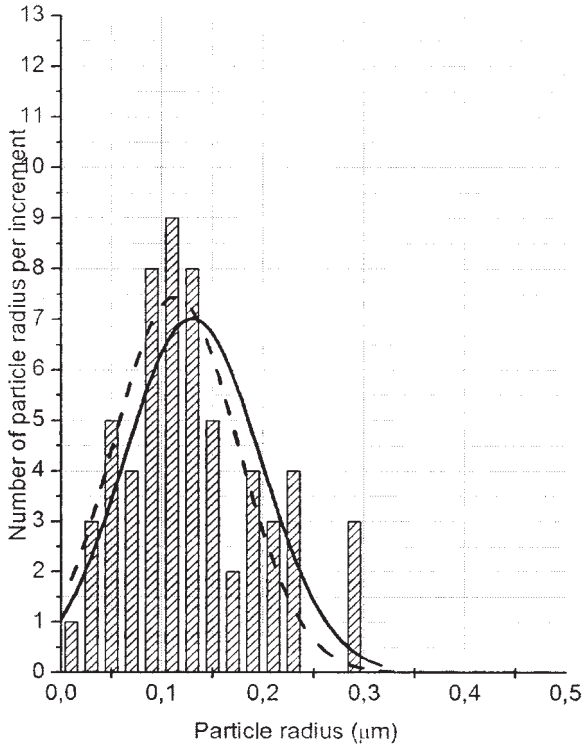

Figure 7 Histogram of a TPU size distribution for a typical TPU/SAN 25/75 blend compatibilized with C2.

Moreover, a narrower distribution of the domain sizes was obtained with the addition of C1c. The size of the dispersed TPU domain increases in blends compatibilized with C2 and C3 if compared with the noncompatibilized blends. This indicates that C2 and C3 do not stabilize morphology against coalescence (Figs. 8 and 9).

Data obtained by means of Gaussian and normal distribution curves as collected in Figure 9 are the values expected when the data deviate from the true value only through a random error. Data obtained as a mean of Gaussian curves are the values expected when the data deviate from the true value only through of random error. We believe that other unpredictable influences (defects occurring during blending and preparation procedures) should also be taken into account. Therefore, it was assumed that data obtained as the mean point of the normal distribution curves truly represent $\bar{r}$ of TPU-dispersed phases.

Rheological properties—-dynamic measurements

For systems where the time–temperature equivalence is valid, the application of the TTS principle[14] allows the estimation of the behavior of polymers in time scales that are not experimentally accessible or only accessible with great difficulty. On the basis of results published by Rush,[43] Kaplan,[16] and Fresko,[15] we applied TTS for noncompatibilized and compatibilized TPU/SAN 25/75 blends. The behavior of these blends is expected to be complex and dominated by the SAN matrix. The shift methods generally assume that all relaxation times of the polymer chain show the same temperature dependence. The Rheometric RheCurve software determines the shift factors empirically. The program calculates the shift factor that gives the best superposition of the data points when multiplied by the frequency of each measurement performed at a given temperature.

Master curves for the storage shear modulus (G') of TPU, SAN, and TPU/SAN 25/75 blends without compatibilizer were constructed from isotherms measured at various temperatures (Fig. 10). The isotherms were measured in the frequency range between 10^2 and 0.01 rad s^{-1}. As reference temperature (T_r) 150°C was chosen. The shift factors for TPU, SAN, and TPU/SAN 25/75 blends are collected in Table III.

TPU has a rheological complex behavior. In spite of an extended measuring range (down to 0.01 rad s^{-1}), no terminal flow region was found at 200°C and above this temperature an extensive decomposition of TPU was observed. At low frequencies, a dependence of approximately $G' \propto \omega^{0.5}$ can be seen, which is typical for phase separated polymers[44,45] of block copolymers i.e., semicrystalline-like region. But in TPU with amorphous phase separated region, G' upturn is due to the phase separated domains, as discussed by Kapnitos.[46] The behavior in the high frequency range seems to be nearly unaffected by the phase separated morphology. Actually, because of the phase separation of soft and hard segments, the dynamic data of TPU cannot be shifted. This can be seen from the temperature depen-

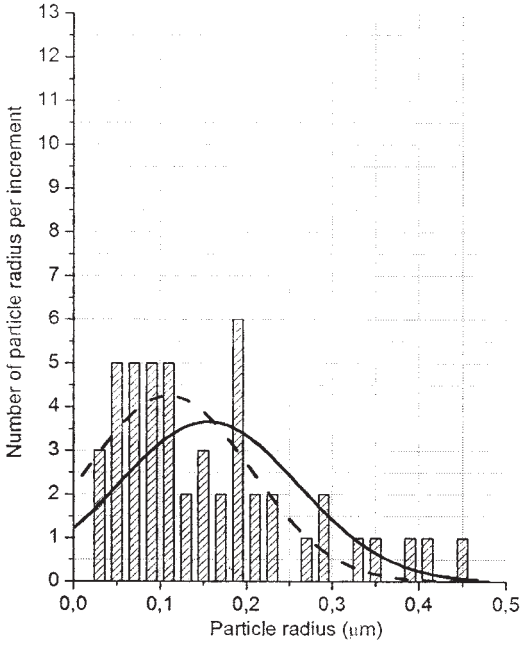

Figure 8 Histogram of a TPU size distribution for a typical TPU/SAN 25/75 blend compatibilized with C3.

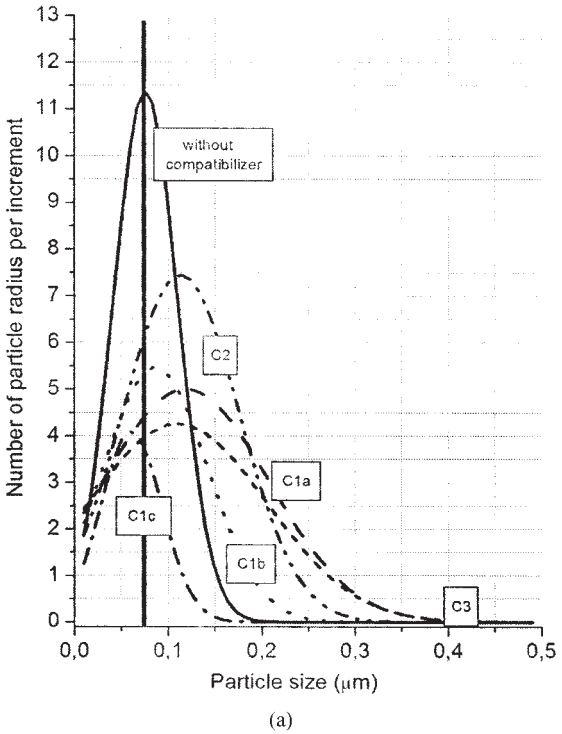

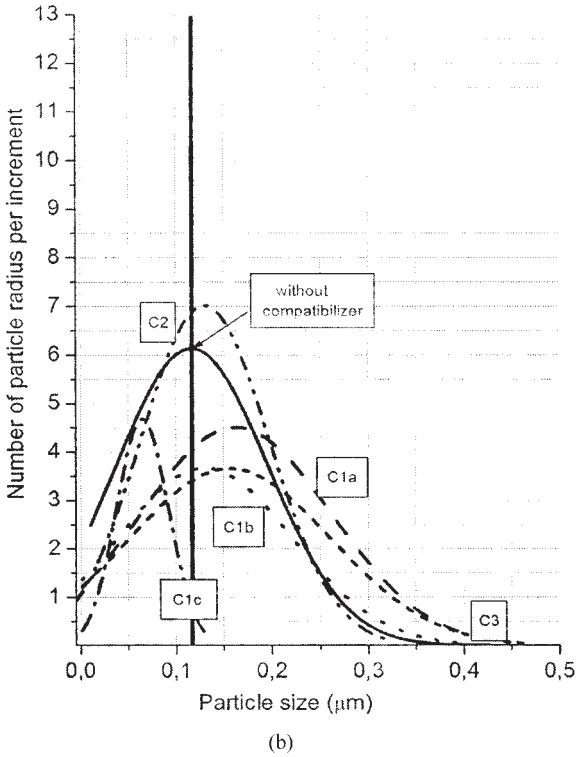

Figure 9 (a) Comparison of Gaussian curves obtained from corresponding micrographs. (b) Comparison of normal curves obtained from corresponding micrographs.

dence of the shift factors (Fig. 11), which do not follow well-known patterns such as Arrehnius or WLF, what was assumed to be due to the presence of two different activation energies relating to the two phase separated domains of TPU.

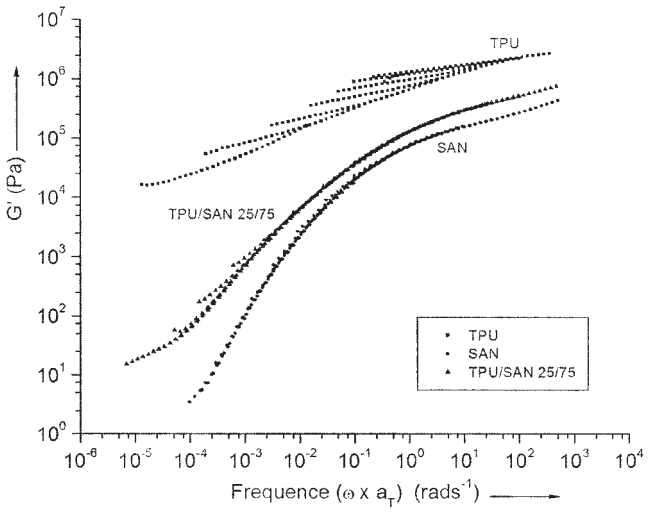

Figure 10 Master curves for the storage shear modulus (G') of TPU, SAN, and TPU/SAN 25/75 blends without compatibilizer.

On the other hand, SAN presents rheologically simple behavior. The master curve shows the plateau at high frequencies and the flow region at low frequencies. The transition from elastic plateau to flow is broad, as is typical for polymers with a broad M_w distribution. Similar results were obtained by Gleisner et al.[47] The curve of the TPU/SAN 25/75 blend lies between the curves of the pure components, but the influence of SAN seems to predominate, as it builds the matrix phase. At high frequencies, the blend behaves very similarly to SAN, as can be seen in the frequency dependent curve as well as in the temperature well as in the temperature dependence of the shift factors. At low frequencies, the behavior is also influenced by TPU that forms the dispersed phase. The storage modulus of the blend is lower than those of TPU and higher than that of SAN through the frequency range. The flow region begins at frequen-

TABLE III
The Thermal Shift Factors (a_T) for TPU, SAN, and TPU/SAN 25/75 Blend with Respect to 150°C

Temperature (°C)	a_T		
	TPU	SAN	TPU/SAN 25/75
130	3.556	—	—
140	2.244	5.056	4.740
150	1.000	1.000	1.000
160	0.512	0.311	0.271
170	0.161	0.0907	0.076
180	0.031	0.0333	0.022
190	0.002	0.0134	0.006
200	$1.3e^{-4}$	0.0058	0.002
210	—	0.0030	$5.21e^{-4}$
220	—	0.002	$2.11e^{-4}$
230	—	$9.7e^{-4}$	$6.69e^{-5}$

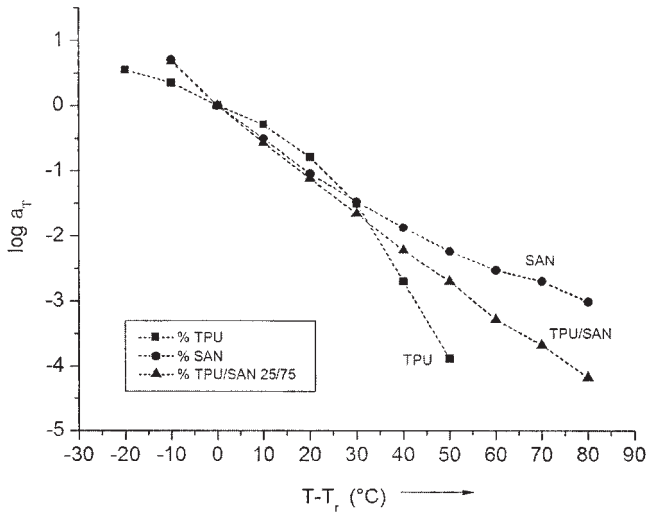

Figure 11 Shift factors for TPU, SAN, and TPU/SAN blends.

cies that are somewhat lower than that observed for the matrix. Such an additional contribution of elasticity is also reported for other immiscible blends.[48–50] Somewhat complex behavior can be observed in the low frequency range of the flow region.

Figure 12 shows the effect of the compatibilizers on the loss shear moduli (G'') of the TPU/SAN 25/75 blends. Master curves of G'' *versus* frequency were obtained by the same procedure, as described previously. The same shift factors for G'' were used and the T_r was 150°C. All master curves show a broad transition from the elastic plateau to the flow region. At high frequencies, there are only small differences between noncompatibilized and compatibilized TPU/SAN 25/75 blends.

Larger changes in the modulus values are observed for blends compatibilized with C1a, C1b as well as C1c. Furthermore, the addition of the PCL homopolymers shifts the flow region to higher frequencies in comparison with the noncompatibilized blend and the blends compatibilized with C2 and C3. A shift to higher frequencies corresponds to lower relaxation times and means that for a given temperature the blends compatibilized with the C1a, C1b as well as C1c will flow within a shorter period.

The shift of the flow region to higher frequencies can be a consequence of changes in the morphology of the blend or of changes in the glass transition temperature (T_g) of the phases, mainly of the phase with the highest T_g. To check the influence of the T_g of the SAN-rich phase on the terminal flow region of the blends, master curves with $T_r = T_g + 50$°C were also constructed from the experimental data (Fig. 13). In this case, it can be found that only the addition of C1c shifts the flow region to higher frequencies, while the addition of other compatibilizers shifts the flow region to even lower frequencies. This indicates that only the blend compatibilized with C1c would have a finer morphology, which means smaller domains of the dispersed phase. This is in agreement with the results

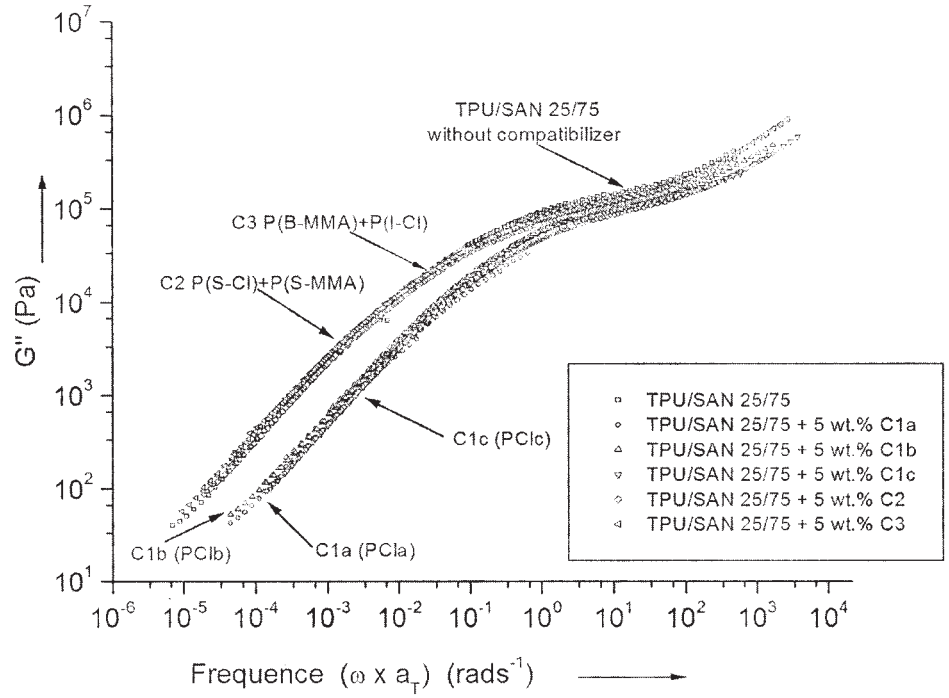

Figure 12 Loss shear modulus (G'') of noncompatibilized and compatibilized TPU/SAN 25/75 blend as a function of the frequency constructed at $T_r = 150$°C.

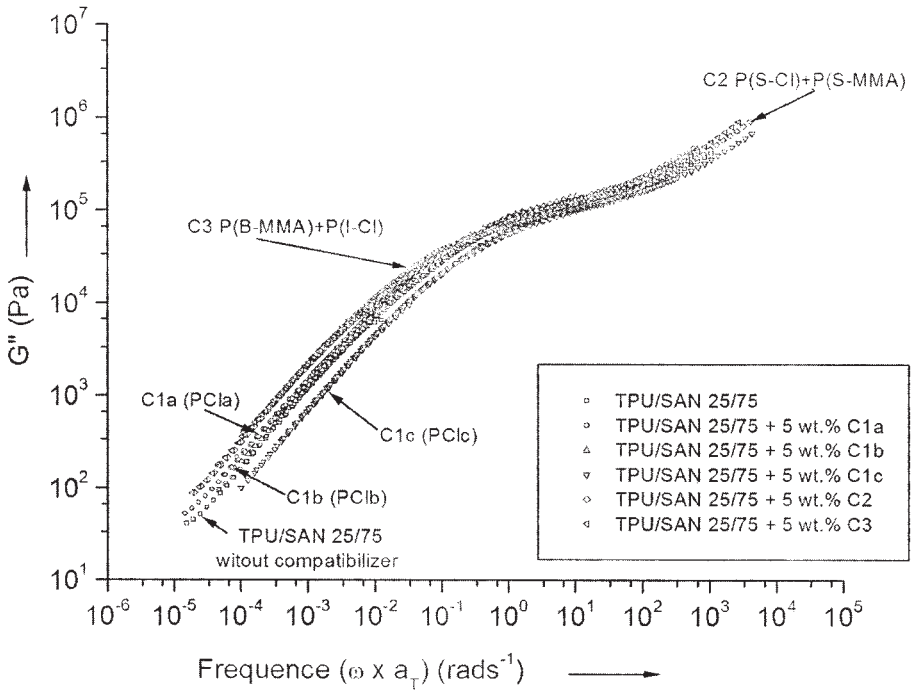

Figure 13 Loss shear modulus (G'') of noncompatibilized and compatibilized TPU/SAN 25/75 blend as a function of the frequency constructed at $T_r = T_g + 150°C$.

of the morphological investigations, as presented in Figure 2(a–f), which clearly show that the size of TPU-rich phase domains for the blend compatibilized with C1c is much smaller than the size of the domains of the other blends.

Rheological properties—-creep experiments

The strain versus time curves of the molten noncompatibilized and compatibilized TPU/SAN 25/75 blends during a creep period of 600 min and the following recovery period of 800 min are shown in Figure 14. All curves were obtained at 140°C. The strain at any time strongly depends on the nature of the compatibilizer. The addition of C2 as well as C3 has only a small influence on the flow properties of the blends, while on the other hand, the addition of C1a, C1b as well as C1c strongly influences their flow behavior.

From the strain curves, the steady-state viscosity (η) and steady state creep compliance (J_e^0) were calculated, as

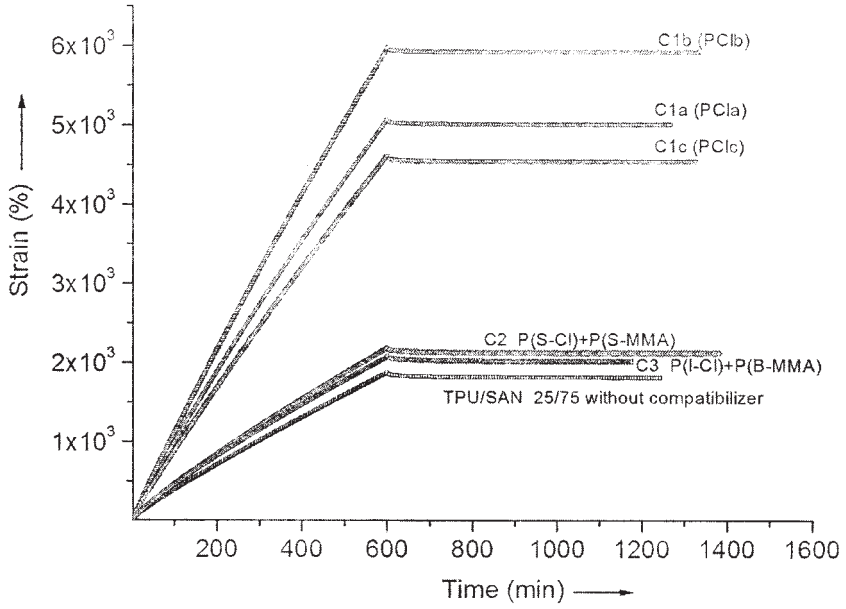

Figure 14 Shear strain of noncompatibilized and compatibilized TPU/SAN 25/75 blends during creep and creep recovery.

TABLE IV
Values of η and J_c^0 of Noncompatibilized and TPU/SAN 25/75 Blends Obtained Using Rhios Software Function Creep Analysis

TPU/SAN 25/75 + 5 wt % compatibilizer	η (Pa s) $\times 10^6$	J_c^0 (Pa^{-1}) $\times 10^{-4}$
none	19.95	0.91
C1a	7.25	1.89
C1b	6.11	1.79
C1c	7.93	1.39
C2	17.48	1.56
C3	18.62	1.77

summarized in Table IV. The addition of any of the compatibilizers increases the value of J_e^0 and decreases the η. While the decrease of η can be ascribed to the share of PCL in the compatibilizers, this is not valid for the increase of J_e^0. However, the molecular weight of the PCL influences both the η and J_e^0. The increase of J_e^0 is the largest for the PCL with the highest M_w. It was assumed that the observed increase of the strain and decrease of the viscosity for the compatibilized blends are mainly related to the decrease of the T_g of the SAN-rich phase in these blends, as found in the dynamic experiments.

Explanation of the experimental pheomena

The TPU/SAN blends compatibilized with C2 and C3 have far too complex structure and are far too complicated to be fully understood. However, the foregoing results showed that poly(ε-caprolactone)s with appropriate M_w improve the compatibility of TPU/SAN blends (smaller domain sizes) and consequently an improvement of some properties of the blends, which were not investigated, can be expected.

In the case of the TPU/SAN blends compatibilized with PCL, at least two driving forces can be postulated that would lead to localization of the compatibilizers at the TPU/SAN interface. Based on simple thermodynamical considerations and as conclusion of presented results, one can expect that the PCL would partition itself into SAN phases. Wu[51] and Korberstein and coworkers[52] showed that the free surface of a miscible blend usually becomes enriched with the component with the lower surface tension, because of the free energy associated with generating a local composition gradient near the surface. By direct analogy, one might expect that the interfacial tension in an immiscible blend, in which at least SAN phase is known to be compatible with PCL, can be lowered by creating a composition gradient at the interface in such a way that the interface itself would be enriched with PCL. On a segmental level, an enrichment of the interface with the PCL compatible with both phases would eliminate some unfavorable interactions acting across it at the expense of some favorable interactions acting within the bulk of each phase.

Second, in the absence of a common component, the immiscible phases will seek to minimize the extent of interpenetrating across the interface by adopting more collapsed conformations in the immediate vicinity of the interface.[42] This is the primary cause of interfacial weakness in immiscible blends. Hence, in the presence of PCL, the blend components could obtain additional degrees of freedom, adopt more favorable conformations, and minimize conformational entropy in the vicinity of the interface if the PCL was located at the interfacial zone and interpenetrated into both phases. Improved molecular interpenetration across the interface leads to better adhesion between phases and consequently to blends properties improvement.

CONCLUSIONS

Morphological investigations of TPU/SAN blends showed that the size of the dispersed TPU domains depends not only on the type and chemical structure of added compatibilizer but also on the compatibilizer's M_w. The presence of 5 wt % of PCL with M_w = 49,000 g mol^{-1} (C1c) strongly reduces the size of the dispersed domains and narrows their distribution, while with all the other compatibilizers an increase of the domain size was observed. In the TEM micrographs of the blend compatibilized with the PCL with M_w = 89,000 g mol^{-1} (C1b), it is possible to recognize that C1b is located at the interface, though no reduction of the domain size is observed. These results lead to the conclusion that C1c and C1b (PCLs with $M_w < 1{,}000{,}000$ g mol^{-1}) act as compatibilizers by decreasing the interfacial tension or by stabilizing the morphology against the coalescence of the phase domains. The M_w of added C1a was probably too high and consequently C1a increased the viscosity of the SAN matrix, which caused the coalescence. The TEM micrographs did not show the independent phases of either PCL in the case of the blend compatibilized with C1a or independent rubber particles in the case of the blend compatibilized with C3, as was assumed on the basis of our previous investigations.[5] It is our speculation that in the case of added C3 compatibilizer components also react with phosphotungistic acid (PTA), which was used for staining the blends and in this way C3 remained undetected in the SAN matrix.

The rheological properties of the molten TPU/SAN 25/75 blends have been investigated both in dynamic and transient mode. The frequency dependent experiments showed that the behavior of the TPU/SAN 25/75 blend was dominated by the SAN matrix, although the influence of the TPU dispersed phase was clearly seen at low frequencies. When a

constant temperature is chosen as reference temperature for the master curves of noncompatibilized and compatibilized blends, the flow regions of all compatibilized blends are shifted to higher frequencies, while when a temperature with constant distance to the highest T_g of the blend is taken as a reference temperature, only the flow region of the blend compatibilized with C1c is shifted to higher frequencies. Taking into account that a shift to higher frequencies is an indication of a finer morphology and that only for C1c smaller domain sizes have been observed with TEM, it was concluded that the differences in T_g have to be taken into account for the construction of the master curves and in the interpretation of the rheological results.

All creep experiments have been performed at 140°C and for all compatibilized blends an increase of the strain at a given time and a decrease of steady state creep compliance (J_e^0) were observed. The effect was more pronounced for the blends compatibilized with C1a, C1b as well as C1c, while the addition of C2 as well as C3 had a weaker influence. Also, a decrease in the recovery time for the blends compatibilized with C1a, C1b as well as C1c was observed. These results were in agreement with the results obtained in the dynamic experiments, when all master curves were constructed at the same reference temperature. To obtain some additional information about the behavior of compatibilized blends in a steady state, the creep measurements should also be performed at temperatures, with a constant distance to the highest T_g of the blend, what is planed in the near future.

In general, improved interphase adhesion was indirectly evidenced from TEM micrographs. It is our speculation that this leads to the better adhesion between phases and consequently to better properties of the compatibilized blends.

Looking from commercial point of view, it is also necessary to point out that the goal of using different compatibilizers is the improvement of the phase adhesion in regard to the mechanical properties. To determine their dependency on the added compatibilizers, the mechanical properties should be also studied in details. Taking into account the known mechanical properties of PCL, it was assumed that PCL itself probably does not improve the mechanical properties of compatibilized blends, what might also show the weak mechanical adhesion between PCL and SAN or TPU, respectively. Thus, the influence of TPU hard segment, which was in this work partly neglected, should also be considered. Finally, a particular advantage for the possible future use of PCL as a compatibilizer for TPU/SAN blends is that this homopolymer can easily be prepared on a commercial scale, principally if its synthesis is compared to the much more troublesome synthesis of high molecular weight block copolymers that are normally used as compatibilizers.

References

1. Datta, S.; Loshe, D. J. Polymeric Compatibilizers: Uses and Benefits in Polymer Blends; Charl Hanser Verlag: Munich, 1996.
2. Ajji, A.; Utracki, L. A. Prog. Rubb Plast Technol 1997, 13, 153.
3. Folkes, S. M. J.; Hope, P. S. Polymer Blends and Alloys; Blackie Academic & Professional: London, 1993.
4. Ulcnik-Krump, M. Ph.D. Thesis, University of Ljubljana, Slovenia, 1999.
5. Ulcnik-Krump, M.; de Lucca Freitas, L. B. Polym Eng Sci 2004, 44, 838.
6. Anastasiadis, S. H.; Gancarz, I.; Koberstein, J. T. Macromolecules 1989, 22, 1449.
7. Shull, K. A.; Kramer, E. J.; Hadziioannou, E. J.; Tang, W. Macromolecules 1990, 23, 4780.
8. Wagner, M.; Wolf, B.A. Polymer 1993, 34, 1460.
9. Tang, T.; Huang, B. Polymer 1994, 35, 281.
10. Noolandi, J.; Hong, K. M. Macromolecues 1982, 15, 482.
11. Sundararaj, U.; Macosko, C. W. Macromolecules 1995, 28, 2647.
12. Favis, B. D. Polymer 1994, 35, 1552.
13. Schlitter, R. R.; Seo, J. W.; Gimzewski, J. K.; Durkan, C.; Saifullah, M. S. M.; Welland, M. E. Science 2001, 292, 1136.
14. Ferry, D. J. Viscoelastic Properties of Polymers, 3rd ed.; Wiley: New York, 1980.
15. Fresko, D. G.; Tschoegl, N. W. J Polym Sci 1971, 35C, 51.
16. Kaplan, D.; Tschoegl, N.W. Polym Sci Eng 1974, 14, 43.
17. Wisniewski, C.; Marin, G.; Monge, P. H. Eur Polym J 1985, 21, 479.
18. Belaribi, C.; Marin, G.; Monge, P. H. Eur Polym J 1986, 221, 481.
19. Zerjal, B.; Malavasic. T. Blends (Thermoplastic Polyurethane-SAN): Polymeric Materials Encyclopedia; CRC Press, Inc: Florida, 1996; Vol. l.
20. Zerjal, B.; Jelcic, Z.; Malavasic, T. Eur Polym J 1996, 32, 1351.
21. Meitzner, E.; Goering, H.; Becker, R. Angew Makromol Chem 1994, 220, 177.
22. Ratzch, M.; Handel, G.; Pompe, G.; Meyer, E. J Macromol Sci A 1990, 27, 1631.
23. Ulcnik, M.; Zerjal, B.; Malavasic, T. Thermochim Acta 1996, 276, 175.
24. Kanapitsas, A.; Pissis, P.; Garcia-Esterella, A.; Ulcnik-Krump, M. IEE Conf. Publ. 430, Dielectric Materials, Measurements and Applications 1996, 430, 230.
25. Van Cleve, R.; Armstrong, G. H.; Simroth, D. W. U.S. Pat. 4, 350, 780 (1982).
26. Jaanarthann, V.; Kessler, J.; Karasz, F. E.; MacKnight, J. Polym Sci; Polym Phys Ed 1993, 32, 1013.
27. Svoboda, P.; Kressler, J.; Ougizawa, T.; Moue, T.; Ozutsumi, K. Macromolecules 1997, 30, 1975.
28. Wang, Z.; Jiang, B. Macromolecules 1997, 30, 6223.
29. Suess, M.; Kressler, J.; Kammer, H. W. Polymer 1987, 28, 957.
30. Cowie, J. M. G.; Lath, D. Macromol Chemie Macromol Symp 1988, 16, 103.
31. Folwer, E. M.; Barlow, J. W.; Paul, D. R. Polymer 1987, 28, 2145.
32. Quintens, D.; Groeninckx, G.; Guest, M.; Aerts, L. Polym Eng Sci 1990, 30, 1488.
33. Eckert-Rectanus, S. Ph.D. Thesis, Johannes Gutenberg University, Mainz, Germany, 1995.
34. Hayat, M. A. Positive Staining for Electron Microscopy; Van Nostrand Reinhold: New York, 1975.
35. Rhios User's Guide; Rheometric Scientific, Inc: New Jersey, 1996.
36. Utracki, L. A. Polymer Alloys and Blends; Hanser Verlag: München, Germany, 1989.
37. Cruz-Orive, L.M. J Macrosc 1976, 107, 235.

38. Sundararaj, U.; Macosko, C. W. Macromolecules 1995, 28, 2647.
39. Exner, H. E.; Hougardy, H. P.; Eds. Quantitative Image Analysis of Microstructures; DGM Informationgesellshaft mbH: Germany, 1988.
40. Wu, S. Polymer 1985, 26, 1855.
41. Wu, S. J Polym Sci Polym Phys Ed 1983, 21, 699.
42. Ghodgaonkar, P. G.; Sundararaj, U. Polym Eng Sci 1996, 36, 1656.
43. Rush, K. C. J Macromol Sci Phys 1968, B2, 421.
44. Bates, F. S. Macromolecules 1984, 13, 1602.
45. Rosedale, J. H.; Bates, S. F. Macromolecules 1990, 23, 2329.
46. Kapnistos, M.; Hinrichs, A.; Vlassiloupols, D.; Anastasiadis, S. H.; Stammer, A.; Wolf, B. A. Macromolecules 1996, 29, 7155.
47. Gleisner, W.; Braun, H.; Friederich, C.; Cantow, H.–J. Polymer 1994, 35, 128.
48. Gramespracher, H.; Meissner, J. J Rheol 1992, 36, 1127.
49. Graebling, D.; Muller, R. J Rheol 1990, 34, 193.
50. Braun, H.; Gleisner, W.; Cantow, H.–J. J Appl Poly Sci 1993, 49, 487.
51. Wu, S. Polymer Interface and Adhesion; Marcel Dekker: New York, 1982.
52. Bhatia, Q. S.; Pan, D. H.; Koberstein, J. T. Macromolecules 1988, 21, 2166.